A Nice Summer at DESY in Hamburg

Summerstudent Program 2009, DESY

Aleksandra Bej[a]
under the supervision of
Markus Diehl

[a] University of Warsaw

This report will describe the time in DESY Hamburg summer 2009

September 10, 2009

Abstract

The experimental studies for the transition form factor of the process $\gamma\gamma^* \to \pi$ agrees with the theoretical concepts for low energy scales (CLEO experiment). This project is about trying to explain the data for higher energy scales (data from BaBar experiment) using the next-to-leading and next-to-next-to-leading order contribiutions for the hard scattering amplitude and leading and next-to-leading order contribiutons for the distribution amplitude evolution. Depending on the order I use the $\overline{\text{MS}}$ and $\overline{\text{CS}}$ scheme

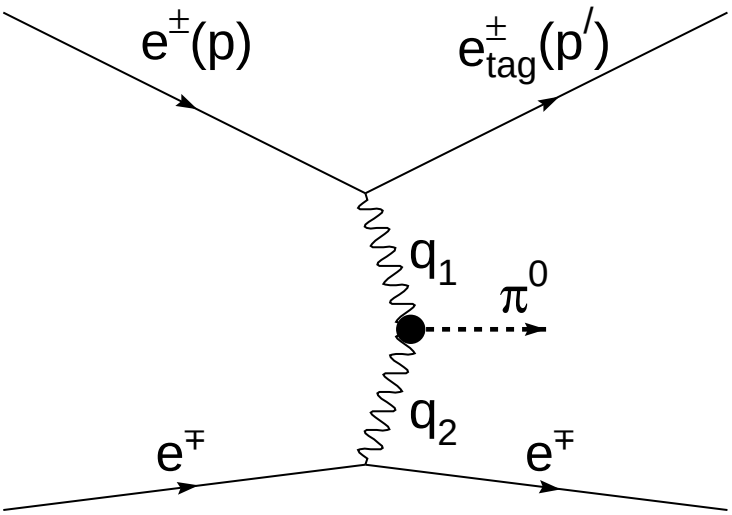

Figure 1: The Feynman graph for the $e^+e^- \to e^+e^-\pi$ process. Figure taken from [3]

The form factor for transitions $\gamma^*\gamma \to \pi$ is a part of the $\gamma^*\gamma\pi$ vertex

$$\Gamma_{\mu\nu} = -ie^2 \mathrm{F}_{\pi\gamma\gamma^*}\left(\overline{Q}\right)\epsilon_{\mu\nu\alpha\beta}\, q^\alpha q'^\beta \tag{1}$$

where $\epsilon_{0123} = 1$, q and q' are respectivelty the photon momenta corresponding to the Lorentz indices μ and ν. The spacelike photon virtualities are
$Q^2 = -q^2, Q'^2 = -q'^2$ as well as

$$\overline{Q}^2 = \frac{1}{2}\left(Q^2 + Q'^2\right) \tag{2}$$

The form factor $\mathrm{F}_{\pi\gamma\gamma^*}\left(\overline{Q}\right)$ is mostly measured as a part of the process $e^+e^- \to e^+e^-\pi$ (see [2], [3]). At large momentum transfer the transition form factor can be represented as a convolution of a calculable hard scattering amplitude with a nonperturbative pion distribution amplitude. We can write the formula up to leading-twist order accuracy (see [1]).

$$F_{\pi\gamma^*}\left(\overline{Q}\right) = \frac{f_\pi}{3\sqrt{2\overline{Q}^2}}\int_{-1}^{1} d\xi \frac{\Phi_\pi\left(\xi,\mu_F\right)}{1-\xi^2}\Big(1 + \frac{\alpha_s\left(\mu_R\right)}{\pi}K\left(\xi,\overline{Q}/\mu_F\right)\Big) \tag{3}$$

where μ_F and μ_R respectively denote the factorization and renormalization scale, and $f_\pi \approx$ 131MeV is pion decay constant. Φ_π is the pion distribution ampilute, which we expand upon Gegenbauer polynomials $C_n^{3/2}\left(\xi\right)$ (the eigenfunctions of the leading order evolution kernel for mesons) in the $\overline{\mathrm{MS}}$ scheme as following

$$\Phi_\pi\left(\xi,\mu_F\right) = \Phi_{AS}\left(\xi\right)\left(1 + \sum_{n=2,4\ldots}^{\infty} B_n\left(\mu_F\right)C_n^{3/2}\left(\xi\right)\right) \tag{4}$$

$$\Phi_{AS}\left(\xi\right) = \frac{3}{2}\left(1-\xi^2\right) \tag{5}$$

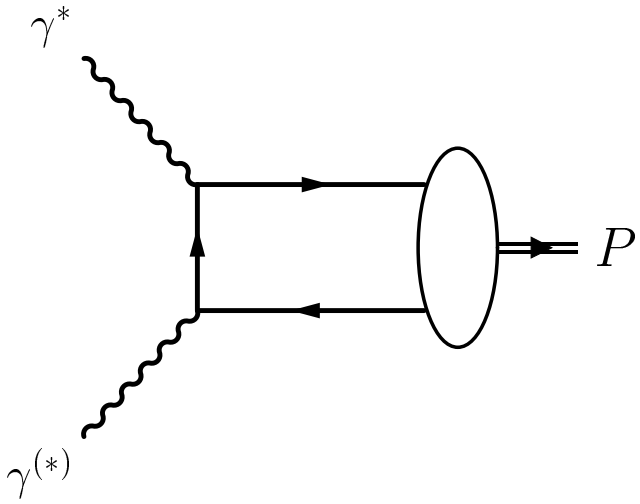

Figure 2: Lowest order Feynman graph for the $\gamma^*\gamma^{(*)} \to \pi$ process. Second graph can be obtained by interchagning the veertices. Figure taken from [1]

Because of the symmetry of the distribution amplitude in ξ the odd contributions vanish.

The B_n coefficents in the leading order evolve according to:

$$B_n(\mu_F) = \left(\frac{\alpha_s(\mu_F)}{\alpha_s(\mu_0)}\right)^{\frac{\gamma_k^{(0)}}{\beta_0}} B_n(\mu_0) \tag{6}$$

where

$$\beta_0 = -\frac{2\mathrm{N}_f}{3} + \frac{11\mathrm{C}_A}{3} \tag{7}$$

Except for the $B_0(\mu_0) = 1$, the $B_n(\mu_0)$ coefficents are complicated to evaluate from theory. Some attempts were made (see for example [4], [5] or [6]) but only with results for $B_2(\mu_0)$. Here we will try to evaluate those coefficents by fitting the form factor function to the experimental data from CLEO and BaBar. This was once done with the CLEO data, but the results don't match the later BaBar data (see figure 3).

Using the Gegenbauer expansion we can rewrite the form factor in a form

$$2\overline{Q}^2 F_{\pi\gamma^*}(\overline{Q}) = \frac{\sqrt{2}f_\pi}{2}\sum_n B_n(\mu_F)\left(2 + \frac{\alpha_s(\mu_r)}{\pi}\mathrm{c}_n(\overline{Q}/\mu_f)\right) \tag{8}$$

where the α_s function was considered in the two-loop order and the $\Lambda_{\overline{MS}} = 350\mathrm{MeV}$ for $N_F = 4$ flavours. The A_n functions can be calculated while knowing the kernel $K(\xi, \overline{Q}/\mu_F)$

$$c_n(\overline{Q}/\mu_f) = \int_{-1}^{1} d\xi\, C_n^{3/2}(\xi)\, K(\xi, \overline{Q}/\mu_F) \tag{9}$$

The explilit formula for the $\overline{\mathrm{MS}}$ scheme and NLO I received is

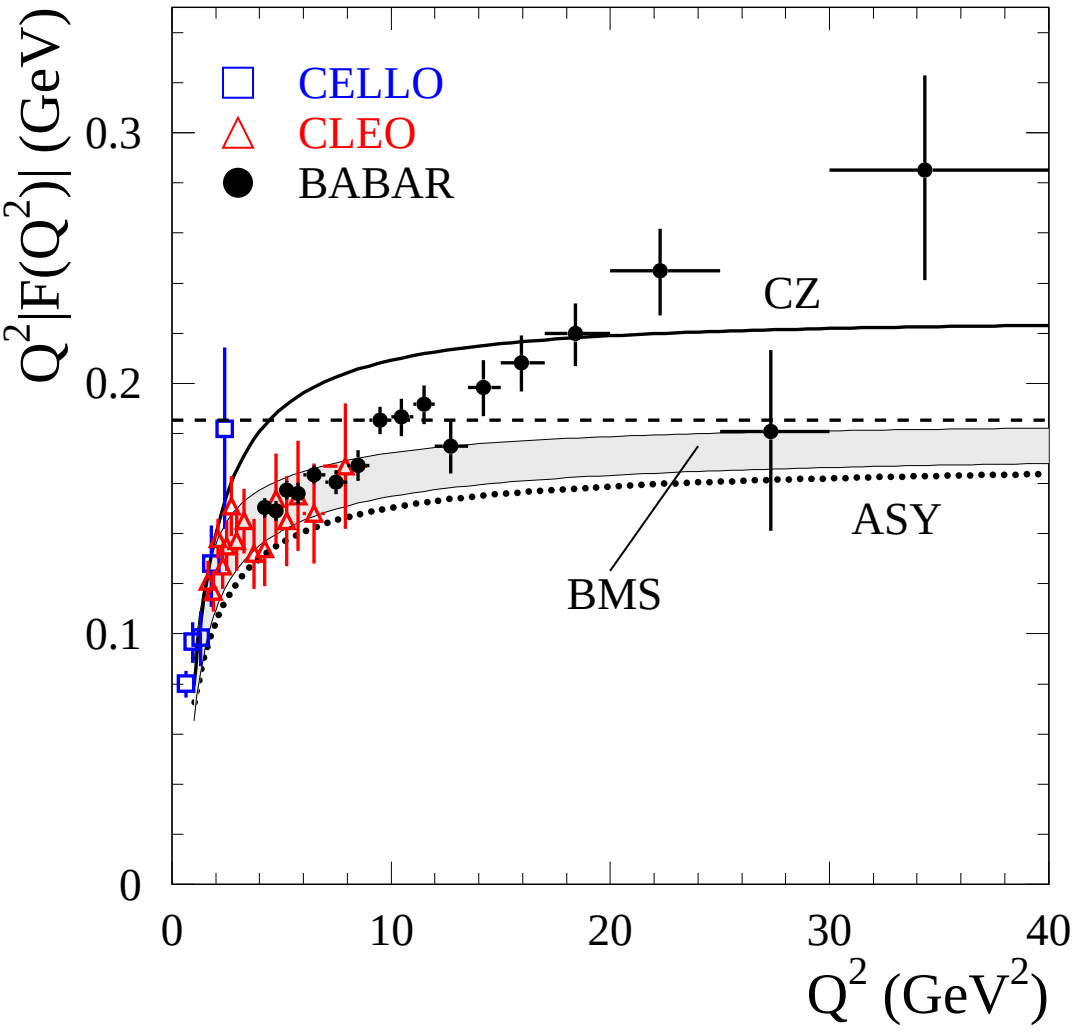

Figure 3: The $\gamma^*\gamma^{(*)} \to \pi$ transition form factor multipied by Q^2. The dashed line indicates the asymptotic limit. The solid and dotted lines show the prediction for the form factor, more details to find in the figure source [3]

$$c_n^{\overline{\rm MS}}\left(\overline{Q}/\mu_f\right) = -3 + 2{\rm Log}\left[2\overline{Q}/\mu_f\right] + \\ +\frac{1}{3}\left(\left(-S_1\left(n+2\right) - S_1\left(n\right)\right)^2 + S_2\left(n+2\right) - S_2\left(n\right)\right) + \\ +\frac{2}{3}\left(-S_1\left(n+2\right) - S_1\left(n\right)\right){\rm Log}\left[2\overline{Q}/\mu_f\right] + \frac{1}{3\left(n+1\right)\left(n+2\right)} \tag{10}$$

where

$$S_j\left(n\right) = \sum_{\rm k=1}^{\rm n} \frac{1}{\rm k^j} \tag{11}$$

Using the kernel from [1] in NLO and calculating the corresponding Gegenbauer moments from equation (9) we have

$$c_0\left(\overline{Q}/\mu_f\right) = -\frac{10}{3} \tag{12}$$

$$c_2\left(\overline{Q}/\mu_f\right) = -\frac{5}{108}\left(-59 + {\rm Log}\left[2\overline{Q}/\mu_f\right]\right) \tag{13}$$

$$c_4\left(\overline{Q}/\mu_f\right) = \frac{10487 - 5460\,{\rm Log}\left[2\overline{Q}/\mu_f\right]}{1350} \tag{14}$$

$$c_6\left(\overline{Q}/\mu_f\right) = \frac{696217 - 287560\,{\rm Log}\left[2\overline{Q}/\mu_f\right]}{58800} \tag{15}$$

$$c_8\left(\overline{Q}/\mu_f\right) = \frac{36387941}{2381400} - \frac{1045}{189}{\rm Log}\left[2\overline{Q}/\mu_f\right] \tag{16}$$

$$c_{10}\left(\overline{Q}/\mu_f\right) = \frac{5265443761}{288149400} - \frac{62816\,{\rm Log}\left[2\overline{Q}/\mu_f\right]}{10395} \tag{17}$$

and all the odd functions are zero. We consider the form factor function with the accuracy up this few A_n funtions, mostly to A_6.

To have a better accuracy of our fit we will also consider the term of the twist-four coupling as

$$-\frac{\rm f_\pi\sqrt{2}\;80}{27}\frac{\delta^2\left(\rm Q^2\right)}{\rm Q^2} \tag{18}$$

where

$$\delta^2\left(\mu^2\right) = \left[\frac{\alpha_s\left(\mu^2\right)}{\alpha_s\left(\mu_0^2\right)}\right]^{\Gamma_{T4}/\beta_0}\delta^2\left(\mu_0^2\right) \tag{19}$$

The coupling $\delta^2\left(\mu^2\right)$ was originally estimated in [8] and found to be
$\delta^2\left(\mu_0^2 = 1{\rm GeV}^2\right) = 0.2 \pm 0.02{\rm GeV}^2$. Details can be found in [9]. The $\Gamma_{T4} = 32/9$

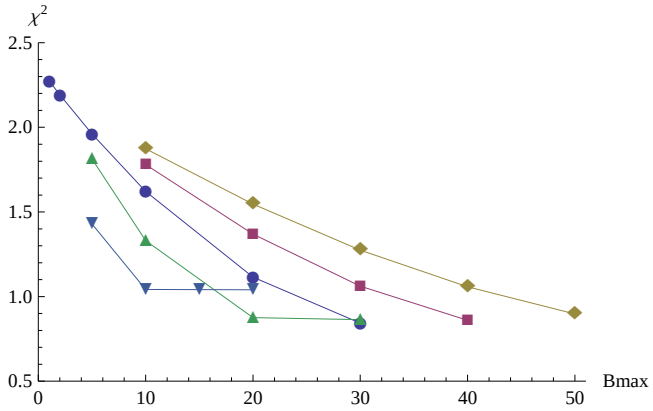

Figure 4: χ^2 results for the $\overline{\text{MS}}$ scheme function depending on the restrictions of the coefficents to fit ($|\text{B}_n(\mu_0)| < \text{B}_{max}$). Fits done with varying μ_F^2 from $\text{Q}^2/4$ to 4Q^2. The highest value series of results correspond to the $\mu_F^2 = 4\text{Q}^2$. The fit were made for $\mu_0 = 2$ and for functions up to A_6

We tried to fit the form factor function to the data to determine the $B_n(\mu_0)$ considering the evolution of $B_n(\mu_F)$ at the LO.

$$\text{Q}^2\text{F}_{\pi\gamma\gamma^*}(\overline{Q}) = \sum_{n=0,2,4...}^{\infty} \text{B}_n(\mu_0)\, A_n^{\overline{\text{MS}}}(\text{Q}, \mu_F, \mu_R) - \frac{\text{f}_\pi\sqrt{2}\ 80}{27}\frac{\delta^2(\text{Q}^2)}{\text{Q}^2} \tag{20}$$

Attempts were made for differently restricted coefficents and varying μ_F and μ_R for the data cut at $Q^2_{\text{min}} = 2\text{GeV}^2$. Figures (4) and (5) are plots of χ^2 in terms of the restriction for coefficents. Fits were made in gnuplot.

We would like the $B_n(\mu_0)$ coefficents to be not bigger in the order than 1, to truncate the formula for the form factor. But one can see, to make a resonable fit they have to be much bigger.

So we continued by going to the higher orders. In $\overline{\text{MS}}$ scheme the evolution of the $B_n(\mu_F)$ in NLO is complicated and includes dependence of the $B_n(\mu_0)$ on $B_{n-1}(\mu_0), ...B_0(\mu_0)$. So the better idea was to change the scheme. In the $\overline{\text{CS}}$ the evolution of $B_n(\mu)$ up to NLO is diagonal

$$B_n(\mu_F) = \left(\frac{\alpha_s(\mu_F)}{\alpha_s(\mu_0)}\right)^{-\frac{\gamma_k^{(0)}}{\beta_0}} \left(1 + \frac{\alpha_s(\mu_F)}{2\pi}\mathcal{A}_n^{(1)}(\mu_F, \mu)\right) B_n(\mu_0) \tag{21}$$

where

$$\mathcal{A}_n^{(1)}(\mu_F, \mu) = \left(1 - \frac{\alpha_s(\mu_F)}{\alpha_s(\mu_0)}\right)\left(-\frac{\beta_1}{2\beta_0}\frac{\gamma_k^{(0)}}{\beta_0} + \frac{\gamma_k^{(1)}}{\beta_0}\right) \tag{22}$$

where $\beta_1 = 102 - 38\text{N}_F/3$. Anomalous dimensions, higher order evolution of B_n coefficents and other details can be found at [7]. But the evolution at NLO gives a very little difference. In figure (6) I plot the ratio of NLO to LO evolution and it is almost one.

But there is a rather big difference in the scattering amplitude. The $\overline{\text{CS}}$ formula for the scattering amplitude one can write as following

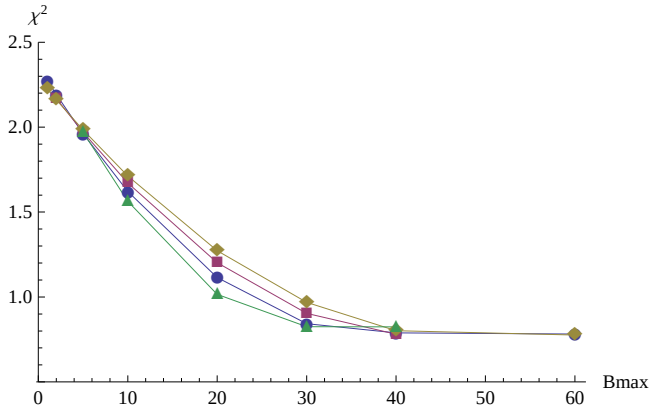

Figure 5: χ^2 results for the $\overline{\text{MS}}$ scheme function depending on the restrictions of the coefficents to fit ($|\text{B}_n(\mu_0)| < \text{B}_{max}$). Fits done with varying μ_R^2 from $\text{Q}^2/2$ to 4Q^2. The highest value series of results correspond to the $\mu_R^2 = 4\text{Q}^2$. The fit were made for $\mu_0 = 2$ and for functions up to A_6

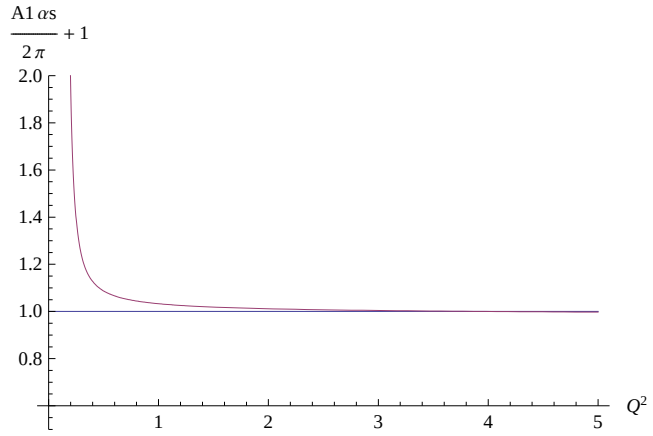

Figure 6: The plot of the NLO to LO ratio, $\left(1 + \frac{\alpha_s(\mu_F)}{2\pi}\mathcal{A}_n^{(1)}(\mu_F, \mu)\right)$ for n = 0 and n = 2 (for $\mathcal{A}_n^{(1)}$ see (22)), for $\mu_0 = 2\text{GeV}$ and $\mu_F^2 = \text{Q}^2$

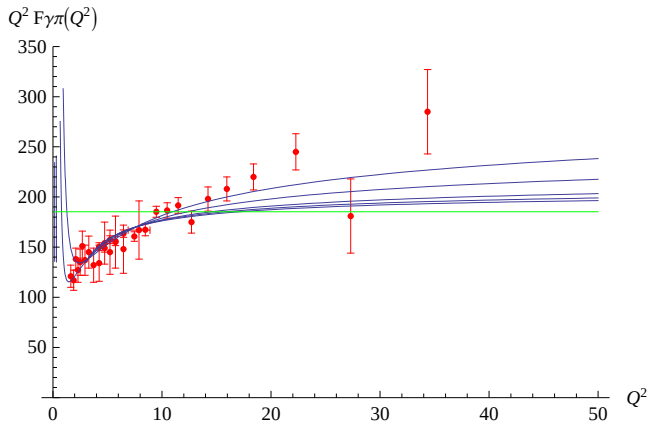

Figure 7: The results for the $\overline{\text{CS}}$ scheme functions in NLO fits. On the plot there are functions $\mathrm{Q}^2 F_{\pi\gamma^*}\left(\mathrm{Q}^2\right)$ with the data from CLEO and BaBar. Various functions depend on the restrictions of the coefficents to fit ($|\mathrm{B}_n\left(\mu_0\right)| \leqslant \mathrm{B}_{max}$). The highest function is for the coefficent restriction of 30, others respectively 15, 5, 2, 1. The results of the χ^2 for those fits can be found in figure 8. Fits were done in gnuplot, for $\mu_0 = 2$ and for functions up to $A_6^{\overline{\text{CS}}(NLO)}$

$$\mathrm{T}_j^{\overline{\text{CS}}}\left(\mathrm{Q},\mu_F\right) = \frac{\sqrt{2}}{3\mathrm{Q}^2}\left(\mathrm{T}_j^{(0)} + \frac{\alpha_s\left(\mu_R\right)}{2\pi}\mathrm{T}_j^{\overline{\text{CS}}(1)}\left(\mathrm{Q}/\mu_F\right)\right) \tag{23}$$

with $\mathrm{T}_j^{(0)} = \frac{3}{2}$ and the

$$\mathrm{T}_j^{\overline{\text{CS}}(1)}\left(\mathrm{Q}/\mu_F\right) = \mathrm{C}_F\left(\mathrm{T}_{F,j}^{\overline{\text{CS}}(1)} + \frac{3}{2}\,\mathrm{Log}\left(\frac{\mathrm{Q}^2}{\mu_F^2}\right)v_j\right) \tag{24}$$

$$v_j = -2S_1\left(j+1\right) + \frac{3}{2} + \frac{1}{\left(j+2\right)\left(j+2\right)} \tag{25}$$

where the numerical values for the first few $\mathrm{T}_{F,j}^{\overline{\text{CS}}(1)}$ are $\mathrm{T}_{F,0}^{\overline{\text{CS}}(1)} = -2.25$, $\mathrm{T}_{F,2}^{\overline{\text{CS}}(1)} = 4.90$, $\mathrm{T}_{F,4}^{\overline{\text{CS}}(1)} = 10.30$, $\mathrm{T}_{F,6}^{\overline{\text{CS}}(1)} = 14.45$, and the explicit formula can be found at [7].

Now the $\mathrm{A}_n^{\overline{\text{CS}}(\text{NLO})}$ have the form

$$\mathrm{A}_n^{\overline{\text{CS}}(\text{NLO})}\left(\overline{Q}/\mu_f\right) = \left(\frac{\alpha_s\left(\mu_F\right)}{\alpha_s\left(\mu_0\right)}\right)^{-\frac{\gamma_k^{(0)}}{\beta_0}}\left(1 + \frac{\alpha_s\left(\mu_F\right)}{2\pi}\mathcal{A}_n^{(1)}\left(\mu_F,\mu\right)\right)\mathrm{T}_n^{\overline{\text{CS}}}\left(\mathrm{Q},\mu_F\right) \tag{26}$$

I did once more a fit to evaluate the B_n coefficents and the results are in figures (8) and (7). As one can see, the fits do not explain well the data for high Q^2 when we restrict the $|\,\mathrm{B}_n\left(\mu_0\right)| \leqslant 1$ and even tor the restriction around 80. Figure 9 shows a fit without any restrictions for the coefficents.

So I continued with the NNLO scattering amplitude expresion in $\overline{\text{CS}}$ scheme.

$$\mathrm{T}_j^{\overline{\text{CS}}}\left(\mathrm{Q},\mu_F\right) = \frac{\sqrt{2}}{3\mathrm{Q}^2}\left(\mathrm{T}_j^0 + \frac{\alpha_s\left(\mu_R\right)}{2\pi}\mathrm{T}_j^{\overline{\text{CS}}(1)}\left(\mathrm{Q}/\mu_F\right) + \frac{\alpha_s^2\left(\mu_R\right)}{4\pi^2}\mathrm{T}_j^{\overline{\text{CS}}(2)}\left(\mathrm{Q}/\mu_F,\mathrm{Q}/\mu_R\right)\right) \tag{27}$$

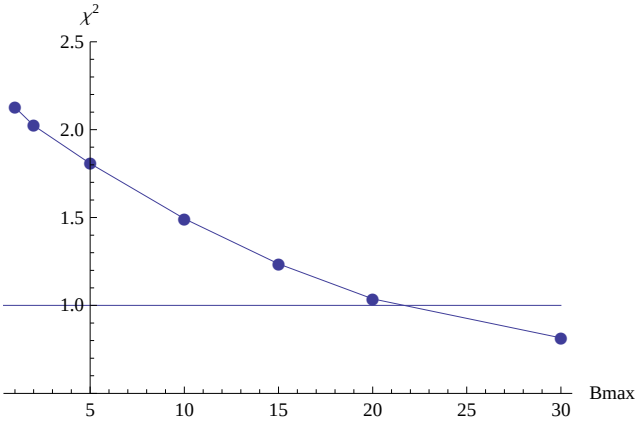

Figure 8: χ^2 results for the $\overline{\text{CS}}$ scheme function depending on the restrictions of the coefficents to fit. Fits were done in gnuplot, for $\mu_0 = 2\text{GeV}$ and for functions up to A_6

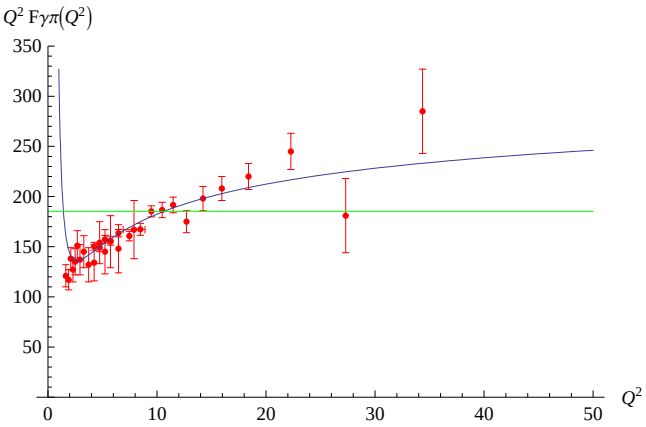

Figure 9: Simple fit for the form factor in $\overline{\text{CS}}$ and NLO in scattering amplitude. The coefficents from the fit are
$\text{B}_2 = 16.7 \pm 2.3$ $\text{B}_4 = -34.9 \pm 5.0$ $\text{B}_6 = 18.5 \pm 2.7$ and the χ^2 is 0.8. There are only present the BaBar data to make the plot more visible

The exact expression for an arbitrary j for the $T_j^{\overline{CS}(2)}$ is very complicated. I used the numerical results that one can find in [7]. In Figure (10) one can find an idea of how do the A_n functions change while changing the scheme or the order.
The NNLO fitting attempts didn't give a good enough result. As before a good fit could be obtained only with high coefficents. In figure (11) and (12) I present an exemplary fit.

(28)

1 Results

For any method I tried, the results were not good enough. Increasing the Q^2_{MIN} from $2\mathrm{GeV}^2$ increased mostly the B_n coefficents in fits. Changing the order and scheme didn't improve the fits also. I didn't manage to explain the experimental results for high Q^2 from BaBar experiment and it seems very unlikely to be done this way.

References

[1] M. Diehl, P. Kroll, C. Vogt, hep-ph/0108220

[2] CLEO Collaboriation, hep-ex/9707031v2

[3] BaBar Collaboration, hep-ex/0905.4778v1

[4] G. Duplancic, A. Khodjamirian, Th. Mannel, B. Melic, N. Offnen, hep-ph/0801.1796v2

[5] A.P. Bakulev, S.V. Mikhailov, N.G. Stefanis, hep-ph/0512119v2

[6] P.Ball, V.M. Braun, A. Lenz, hep-ph/060363v1

[7] B. Melic, D.Muller, K. Passek-Kumericki, hep-ph/0212346

[8] V.A. Novikov, M.A. Shifman, A.I. Vainshtein, M.B. Voloshin, and V.I. Zakharov, Nucl. Phys B237, 525 (1984)

[9] A.P. Bakulev, S.V. Mikhailov, hep-ph/0212250v3

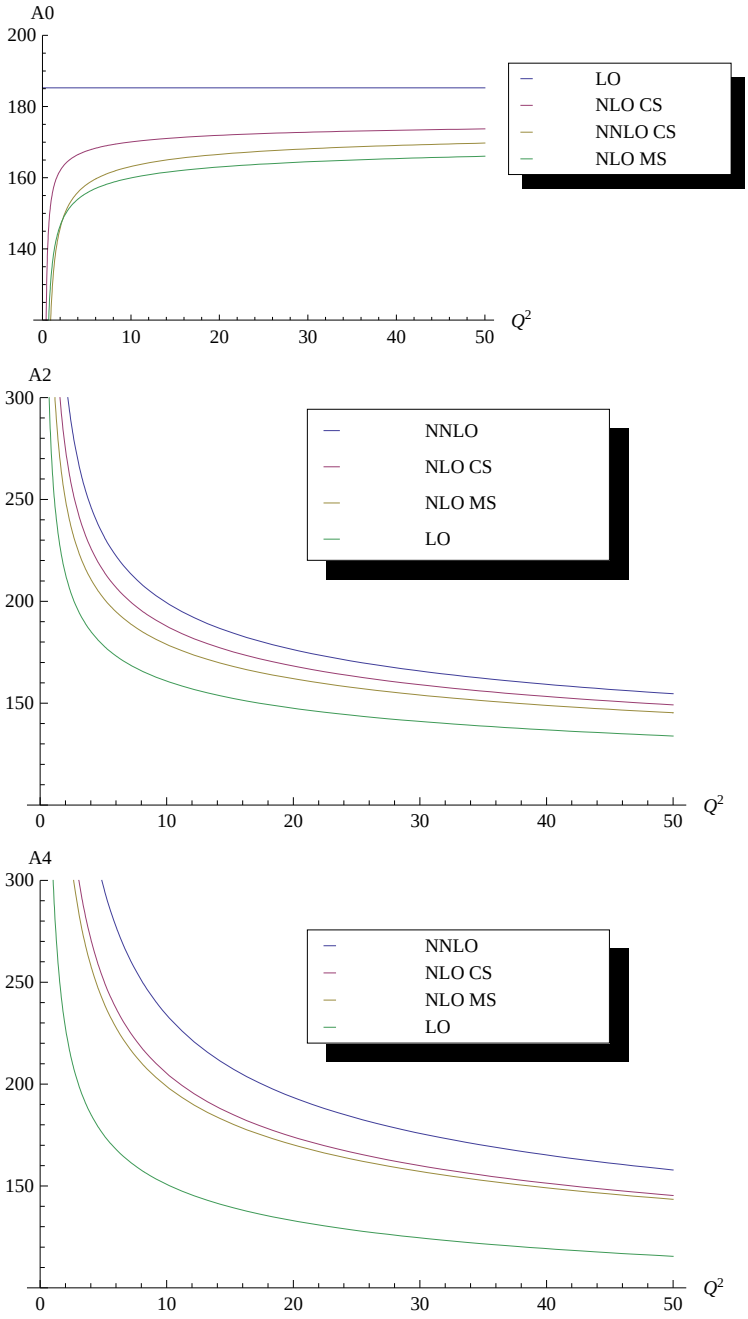

Figure 10: Results for different schemes and orders. The legend is on the form: order of the scattering amplitude, order of the disribution amplitude evoltion , scheme. Plots done for $\mu_0 =$ 2GeV and $\mu_F = \mu R =$ Q

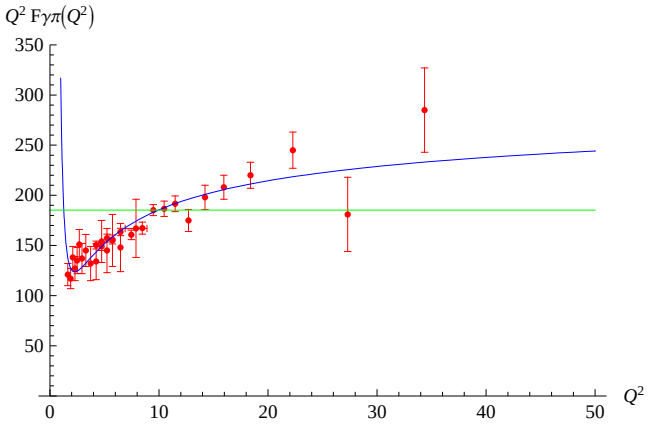

Figure 11: Form factor function fit for $\mu_0 = 2\text{GeV}$ and $\mu_F^2 = \mu R^2 = \text{Q}^2$.The coefficents from the simple fit done in Mathematica are: $\text{B}_2 = 10.3$ $\text{B}_4 = -19.5$ $\text{B}_6 = 9.6$

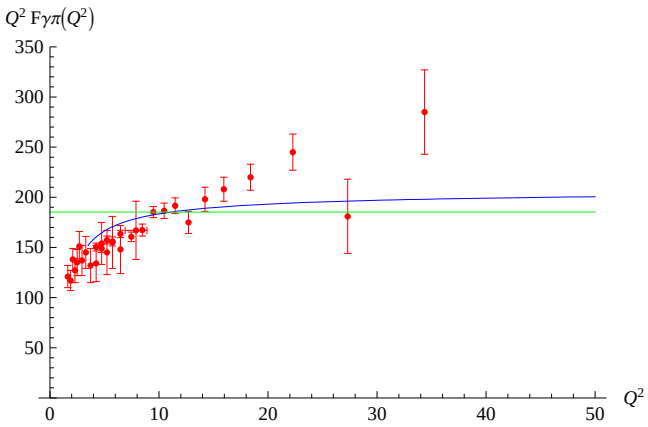

Figure 12: Form factor function fit for $\mu_0 = 2\text{GeV}$ and $\mu_F^2 = \mu R^2 = \text{Q}^2$. The coefficents from the simple fit done in Mathematica are: $\text{B}_2 = 0.85$ $\text{B}_4 = -0.64$